APPLIED AND ENVIRONMENTAL MICROBIOLOGY, Nov. 2009, p. 6655–6661 Vol. 75, No. 21
0099-2240/09/$12.00 doi:10.1128/AEM.01260-09

Processivity, Synergism, and Substrate Specificity of *Thermobifida fusca* Cel6B▽

Thu V. Vuong and David B. Wilson*

Department of Molecular Biology and Genetics, Cornell University, Ithaca, New York 14853

Received 1 June 2009/Accepted 25 August 2009

A relationship between processivity and synergism has not been reported for cellulases, although both characteristics are very important for hydrolysis of insoluble substrates. Mutation of two residues located in the active site tunnel of *Thermobifida fusca* exocellulase Cel6B increased processivity on filter paper. Surprisingly, mixtures of the Cel6B mutant enzymes and *T. fusca* endocellulase Cel5A did not show increased synergism or processivity, and the mutant enzyme which had the highest processivity gave the poorest synergism. This study suggests that improving exocellulase processivity might be not an effective strategy for producing improved cellulase mixtures for biomass conversion. The inverse relationship between the activities of many of the mutant enzymes with bacterial microcrystalline cellulose and their activities with carboxymethyl cellulose indicated that there are differences in the mechanisms of hydrolysis for these substrates, supporting the possibility of engineering Cel6B to target selected substrates.

Cellulose is a linear homopolymer of β-1,4-linked anhydrous glucosyl residues with a degree of polymerization (DP) of up to 15,000 (5). Adjacent glucose residues in cellulose are oriented at an angle of 180° to each other, making cellobiose the basic unit of cellulose structure (5). The β-1,4-glycosidic bonds of cellulose are enzymatically hydrolyzed by three classes of cellulases. Endocellulases (EC 3.2.1.4) cleave cellulose chains internally, generating products of variable length with new chain ends, while exocellulases, also called cellobiohydrolases (EC 3.2.1.91), act from one end of a cellulose chain and processively cleave off cellobiose as the main product. The third class is the processive endocellulases, which can be produced by bacteria (2, 20).

Processivity and synergism are important properties of cellulases, particularly for hydrolysis of crystalline substrates. Processivity indicates how far a cellulase molecule proceeds and hydrolyzes a substrate chain before there is dissociation. Processivity can be measured indirectly by determining the ratio of soluble products to insoluble products in filter paper assays (14, 19, 39). Although this approach might not discriminate exocellulases from highly processive endocellulases (12), it is very helpful for comparing mutants of the same enzyme (19). The processivity of some glycoside hydrolases also can be determined from the ratio of dimers to monomers in the hydrolysate (13).

Four types of synergism have been demonstrated in cellulase systems: synergism between endocellulases and exocellulases, synergism between reducing- and nonreducing-end-directed exocellulases, synergism between processive endocellulases and endo- or exocellulases, and synergism between β-glucosidases and other cellulases (3). Synergism is dependent on a number of factors, including the physicochemical properties of the substrate and the ratio of the individual enzymes (10).

Great effort has been focused on improving enzymatic hydrolysis of cellulases in biomass (24). However, studying biomass is difficult due to its complexity; instead, nearly pure cellulose, amorphous cellulose, or carboxymethyl cellulose (CMC) are commonly used as substrates (22).

Random mutagenesis approaches and rational protein design have been used to study cellulose hydrolysis (18), to improve the activity of catalytic domains and carbohydrate-binding modules (19), and to thermostabilize cellulases (9). Increased knowledge of cellulase structures and improvements in modeling software (1) have facilitated rational protein design. The structures of five glycoside hydrolase family 6 cellulases from four microorganisms, *Trichoderma reesei* (23), *Thermobifida fusca* (26), *Humicola insolens* (6, 29), and *Mycobacterium tuberculosis* (30), have been determined. Structural analysis showed that the active sites of the exocellulases are enclosed by two long loops forming a tunnel, while the endocellulases have an open active site groove. Movement of one of these loops is important for enzymatic activity (6, 35, 37).

In nature, as well as for industrial applications, mixtures of cellulase are required; therefore, a better strategy for designing individual enzymes to improve the activity of mixtures is critical. In this study, we used Cel6B, a nonreducing-end-directed, inverting exocellulase from *Thermobifida fusca*, a thermophilic soil bacterium, as a model cellulase to investigate the impact of improved exocellulases in mixtures with endocellulases since *T. fusca* Cel6B is important for achieving the maximum activity of synergistic mixtures (35). Cel6B activity is similar to that of the fungal *T. reesei* exocellulase Cel6A, but Cel6B has higher thermostability and a much broader pH optimum (36). Six noncatalytic residues in the active site tunnel of *T. fusca* exocellulase Cel6B were mutated to obtain insight into the role of these residues in processivity and substrate specificity. Two mutant enzymes that showed higher activity with filter paper and processivity were investigated further for production of oligosaccharides and synergism to analyze the relationship between processivity and synergism.

* Corresponding author. Mailing address: 458 Biotechnology Building, Cornell University, Ithaca, NY 14850. Phone: (607) 255-5706. Fax: (607) 255-2428. E-mail: dbw3@cornell.edu.

▽ Published ahead of print on 4 September 2009.

MATERIALS AND METHODS

Site-directed mutagenesis and enzyme purification. The entire Cel6B gene in plasmid pSZ143 (35) was used as the template for mutagenesis. Complementary primers were designed using PrimerSelect (DNASTAR Lasergene v.8.0) to incorporate the desired mutations. PCR was performed for 18 cycles consisting of 95°C for 1 min, 60°C for 50 s, and 68°C for 7 min, using the QuikChange method (Agilent Technologies). PCR products were transformed into *Escherichia coli* DH5α, and mutant plasmids were checked by DNA sequencing (Applied Biosystems 3730 automated DNA analyzer at Life Sciences Core Laboratories Center, Cornell University). Correct mutant plasmids were transformed and expressed in *E. coli* BL21 RPIL DE3 (Agilent Technologies).

Wild-type and mutant enzymes were purified using previously described chromatographic techniques (36). Cel6B concentrations were calculated from optical densities at 280 nm using an extinction coefficient (ε) of 15,000 $M^{-1} \cdot cm^{-1}$ calculated from the amino acid composition. *T. fusca* Cel5A and Cel48A used for synergism were purified by chromatographic techniques as previously described (15, 16).

Polysaccharide assays. As recommended by Ghose (7), polysaccharide assays were conducted using a series of enzyme concentrations greater and less than the target digestion concentration for each substrate for a fixed time with a saturating amount of substrate (7). Enzymatic activities were determined using 2.5-mg/ml bacterial microcrystalline cellulose (BMCC) and phosphoric acid-swollen cellulose (SC), as well as 8-mg/ml Whatman no. 1 filter paper (FP). Enzymes were also tested using 2.5-mg/ml phosphoric acid-treated cotton (PC) that was prepared for this study using a previously described method for swollen cellulose (38). All assays were performed using a 0.4-ml reaction mixture in triplicate for 16 h at 50°C in the presence of 50 mM sodium acetate (NaOAc) (pH 5.5). Reducing sugars were measured using dinitrosalicylic acid (7), as suggested by Li et al. (19). KaleidaGraph (Synergy Software) was used to fit the curve to determine the amount of enzyme required for 6% substrate digestion. As the activity with FP was low, enzyme activity was calculated using 1.5 μM enzyme.

The distribution of reducing ends in the supernatant (soluble) and in FP (insoluble) was measured to calculate processivity (14).

Synergism assays. Synergism assays for wild-type and selected mutant enzymes were performed in the presence of *T. fusca* Cel5A and/or Cel48A using FP and PC at different molar ratios. Synergism was measured based on the amount of enzyme needed to obtain 5% digestion of FP or 6% digestion of PC in 16 h at 50°C. The synergistic effects were calculated using the activity of the mixture divided by the sum of the individual activities.

Substrate binding assays. Binding of 4 μM enzyme to 0.1% BMCC was determined in 50 mM NaOAc buffer (pH 5.5) and 10% glycerol. Reaction mixtures were incubated at 4°C (to eliminate hydrolysis) for 1 h on a Nutator rocking table (Clay-Adams); the optical density at 280 nm was measured to determine the amount of unbound protein from the supernatant, which was then used to calculate the percentage of each enzyme bound.

TLC. Thin-layer chromatography (TLC) was performed as previously described (17).

HPLC analysis. HPLC was conducted using Shimadzu HPLC equipment consisting of an LC-20AD pump, an SIL-20A autosampler, and an RID-10A refractive index detector. Separation was achieved using an Aminex HPX-87P analytical column (300 mm by 7.8 mm; Bio-Rad) equipped with Micro-Guard deashing cartridges (Bio-Rad). The column oven temperature was 84°C. Fifty picomoles of enzyme was incubated with 3.2 mg of FP or 500 nmol of cellotriose (G3 [three glucose molecules]) (Megazyme) for 16 h or with 10 nmol of cellohexaose (G6) (Megazyme) for 10 min in 400 μl of 50 mM NaOAc (pH 5.5) at 50°C. The samples were filtered through Millipore 5K NMWL membrane filter devices before they were injected at a rate of 0.6 μl/min. Data were analyzed using OriginPro v.8.0 (Origin Lab).

CD analysis. Spectra for 10 μg/μl protein were recorded from 190 to 290 nm with an Aviv CD400 spectrometer (Aviv Biomedical, Inc.) at a scanning rate of 1 nm/s at 4°C. The circular dichroism (CD) spectra were analyzed to determine the percent secondary structure using the CDNN CD spectra deconvolution software developed by Bohm et al. (4).

Thermostability assays. Cel6B wild-type and selected mutant enzymes were preincubated in 50 mM NaOAc (pH 5.5) at temperatures ranging from 45°C to 70°C for 16 h, and then 1.5 μM enzyme was assayed with SC at 50°C for 16 h to calculate the temperature at which activity dropped by 50% (T_{50}).

RESULTS

Selection of mutations. Residues for mutation were chosen by analysis of the structures of *H. insolens* Cel6A (1OCB.pdb), *T. reesei* Cel6A (1QK2.pdb), and *T. fusca* Cel6A (2BOD.pdb), as well as a structural model of the Cel6B catalytic domain, which was built based on the X-ray structures of *H. insolens* Cel6A using the Swiss-Model Workspace. The reliability of the model was evaluated by the WhatCheck program (11).

Figure 1 shows the location of the residues chosen for mutation. N282 and R180 are located at the +2 and −4 glucose subsites, respectively, whereas L230 is located in a turn on the top of the tunnel. The potential sugar-binding residues N282 and R180 were mutated to investigate the role of residues near the tunnel entrance and exit in processivity. W464, which corresponds to W371 in *H. insolens* Cel6A, was suggested previously to participate in substrate binding (28), while residues D512 and M514 might affect loop flexibility.

Enzyme activity and processivity. All the mutant enzymes behaved like wild-type Cel6B during purification. The CD spectra of all mutant enzymes except the M514A and M514Q enzymes (see Fig. 3) were identical to that of wild-type enzyme, indicating that the global secondary structure of the mutant proteins remained intact.

The purified enzymes were assayed using five polysaccharides, and their activities were expressed as percentages of the wild-type activity to facilitate comparison (Table 1). BMCC and FP, which is made from long-fiber cotton pulp, are crystalline substrates with a DP of >1,000 (27), but BMCC has a larger surface area and is more reactive (10). Both PC and SC are amorphous celluloses with DP of approximately 1,500 and 2,600, respectively; PC showed lower crystallinity and crystallite size than SC (Jessica Hatch, personal communication). CMC is a soluble substrate consisting of β-1,4-glucose units with random carboxylmethyl substitutions and a DP of 250 to 500 (25).

Mutant enzymes with mutations in residues near the tunnel exit (R180K and R180A) and the tunnel entrance (N282A and N282D) had, on average, a twofold increase in processivity (Table 1). The L230A mutation slightly increased processivity and increased the activity with PC over 250% (Table 1). HPLC was used to investigate the production of oligosaccharides by the N282A and L230A enzymes with FP. While cellobiose (G2) is the main product, small amounts of cellotriose (G3) and glucose (G1) were also produced (Table 2). As cellobiose is the repeating unit of cellulose (5), it is thought that the first hydrolytic step can produce either G3 or G2, but the subsequent steps yield only G2. TLC and HPLC of the products of G3, G4, G5, and G6 hydrolysis showed that G4, G5, and G6 were completely hydrolyzed within minutes, while a small amount of G1 was detected for G3 hydrolysis after 16 h of incubation (data not shown). Therefore, the (G2 − G1)/(G3 + G1) ratio also can provide an estimate of processivity. Both the N282A and L230A mutant enzymes produced approximately 2.5-fold more oligosaccharides than the wild-type enzyme, and their (G2 − G1)/(G3 + G1) ratios were 1.8-fold higher (Table 2). However, when hydrolyzing G6, the N282A enzyme was less active and produced a lower ratio of G2 to G3 than the L230A enzyme (Table 2).

Synergism with other *T. fusca* enzymes. The L230A and N282A mutant enzymes were assayed in the presence of *T. fusca* endocellulase Cel5A to test for synergism in FP hydrolysis at a molar ratio of Cel6B to Cel5A of 4:1, which was previously found to be optimal (14, 33). Although the activities

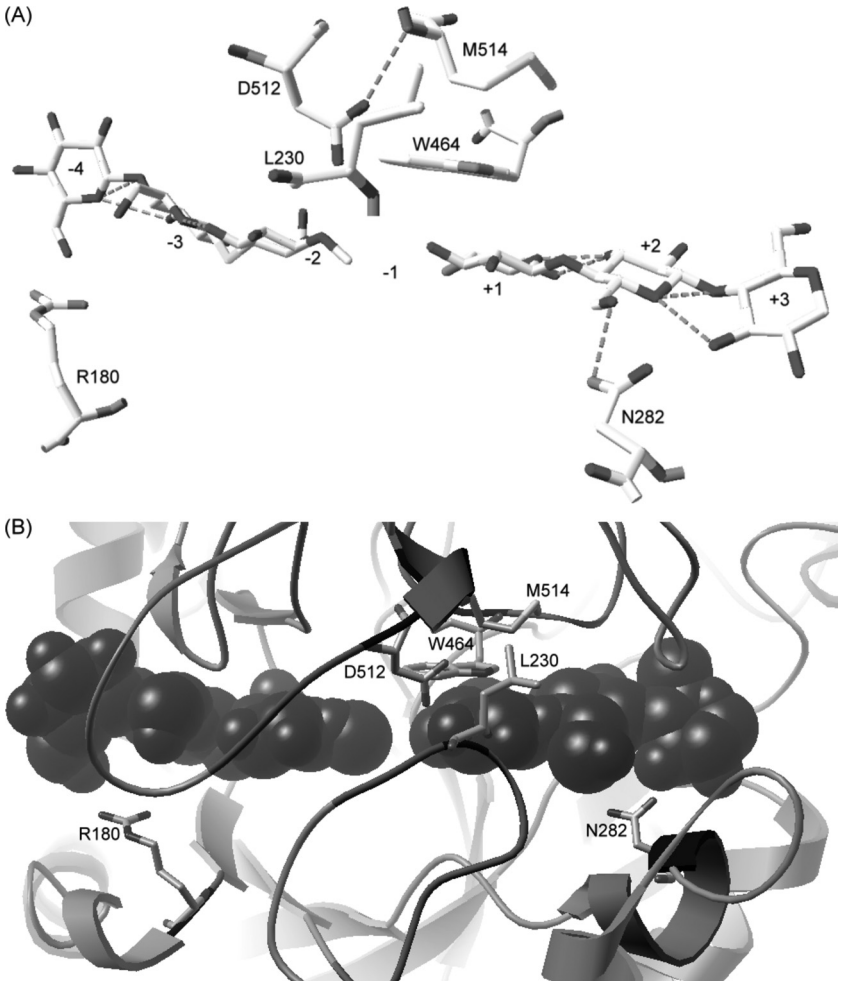

FIG. 1. Location of *T. fusca* Cel6B residues for mutation, modeled using *H. insolens* Cel6A (1OCB.pdb; 1.75-Å resolution) by the Swiss-Model Workspace. (A) One-dimensional view. Dashed lines show hydrogen bonds. (B) Three-dimensional view, showing the active site tunnel with two molecules of fluoresceinylthioureido-derivatized tetrasaccharide (for neatness, the +4 glycosyl residue was removed).

of these individual mutant enzymes with FP were around 150% of the wild-type activity, mixtures of them with Cel5A did not exhibit higher activity than the mixture containing the wild-type enzyme (Table 3). A similar pattern was observed at two different molar ratios (9:1 and 19:1) and for a range of incubation times (4 to 16 h), as well as with mixtures with *T. fusca* Cel9A-68, a processive endocellulase (data not shown). The same result was observed for mixtures of Cel6B with Cel5A for PC hydrolysis. Although the N282A mutant enzyme alone exhibited over 310% of the wild-type activity with PC, the activity of the mixture was only 63% of that of the mixture containing the wild type (Table 3). Processivity with PC was not reported due to difficulty in measuring insoluble reducing sugars from this substrate.

To test the correlation between processivity and synergism, the processivity of the mixtures was measured. Mixtures of mutant enzymes with Cel5A showed lower processivity than mixtures with the wild-type enzyme (Table 3). Cel6B mutant enzymes were also mixed with *T. fusca* Cel48A, an exocellulase that attacks the reducing end of cellulose. The Cel6B mutant enzymes, which individually showed higher processivity, exhibited higher synergism and processivity with Cel48A than the mixture containing the wild-type enzyme (Table 3).

Substrate specificity. The W464A and W464Y mutant enzymes had reduced activity with BMCC but had higher activity with PC and CMC (Table 1). The binding of the W464A enzyme to BMCC was lower than that of the wild-type enzyme (Fig. 2). The activity of the W464A enzyme with CMC increased sevenfold, and that of the W464Y enzyme was nearly double. High activity of the W464A mutant enzyme with CMC was also observed with lower concentrations of CMC (0.25 and 0.5%) (data not shown). TLC analysis confirmed the high activity of this enzyme with CMC and showed that the products were not changed by the mutation (data not shown).

The activity of the two M514 mutant enzymes with BMCC unexpectedly decreased with increasing time of storage (in 5 mM NaOAc [pH 5.5] and 10% glycerol at −70°C). BMCC assays conducted right after purification showed that the mutant enzymes had slightly higher activities than the wild-type enzyme (Table 1); 5 months after the first enzymatic assay, the M514A enzyme specific activity was approximately 2% of the

TABLE 1. Activities and processivity of the Cel6B mutant enzymes with polysaccharide substrates

Enzyme	% of wild-type activity with[a]:					Processivity
	BMCC	SC	PC	CMC	FP[b]	
Wild type	100	100	100	100	100	7.2
Mutant enzymes for processivity						
R180A	85	125	130	96	91	16.4
R180K	59	123	180	104	100	13.6
L230A	108	137	252	126	159	9.9
N282A	105	86	313	196	145	20.9
N282D	116	110	323	158	145	13.1
Mutant enzymes for substrate specificity						
W464A	26	86	368	718	132	7.9
W464Y	54	79	159	195	114	8.9
D512A	34	174	240	568	95	5.7
M514A[c]	131	131		151	91	5.9
M514Q[c]	125	128		174	118	9.1

[a] Activity was calculated for 6% digestion for BMCC, SC, and PC and for 1.5% digestion for CMC. The average coefficients of variation were 4, 5, 5.5, 2.5, 3, and 4% for activities with BMCC, SC, PC, CMC, and FP and processivity (soluble reducing sugars/insoluble reducing sugars), respectively. The activities of the wild-type enzyme with BMCC, SC, PC, CMC, and FP were 0.93, 2.25, 3.37, 0.57, and 0.22 μmol cellobiose min^{-1} μmol^{-1} enzyme, respectively.

[b] Activity was calculated with 1.5 μM enzyme.

[c] Activity was measured right after purification when PC had not been prepared yet.

wild-type activity (data not shown). The loss of activity of the M514A enzyme with BMCC correlated with increased activity with CMC, and the loss of enzymatic activity of the M514A enzyme was always greater than that of the M514Q enzyme (data not shown). Sodium dodecyl sulfate-polyacrylamide gel electrophoresis gels showed that there was no difference in mobility or band pattern between boiled and unboiled samples of the wild-type and mutant enzymes (data not shown), eliminating the possibility of enzymatic degradation during storage. Both mutant enzymes were unstable at 55°C and higher temperatures; their T_{50} was 58°C, while the T_{50} of the wild-type enzyme was 64°C (data not shown). CD analysis after 2 years of storage showed that the M514A enzyme spectrum, particularly from 207 to 228 nm, and the M514Q spectrum from 260 to 290 nm are different from the wild-type spectrum, indicating that there is structural modification of each enzyme (Fig. 3A). CD spectrum analysis indicated that the α-helix content of the M514A mutant enzyme was higher than that of the wild type, while the content of random coils was slightly lower than that of the wild type (Fig. 3B).

DISCUSSION

Link between processivity and synergism. Mutation of either N282 or R180, which are at opposite ends of the active site tunnel, to an amino acid with shorter side chains increased the processivity of Cel6B, and mutation to the smallest side chain (Ala) gave the largest increase. Each subsite of a cellulase can accommodate both faces of the pyranoside ring and tolerate the C_6 hydroxyl group when the substrate moves along the catalytic site (28). The decrease in the size of the side chains at these positions might allow the cellulose molecule more freedom to advance through the tunnel in the case of the N282A mutant enzyme and facilitate the release of cellobiose for the R180A mutant enzyme. A study of *Aspergillus niger* endopolygalacturonases also showed that a region far from the scissile bond (subsite −5) strongly influences processivity (21). High processivity does not always indicate higher activity, as observed for the FP activity of the R180 mutant enzymes; processivity is more about disassociation than about the rate of hydrolysis.

Increased processivity of the N282A mutant enzyme also was shown by its high (G2 − G1)/(G3 + G1) ratio. Although the processivity of the N282A mutant enzyme as measured by the ratio of soluble reducing sugars to insoluble reducing sugars was higher than that of the L230A mutant enzyme, the oligosaccharide ratios of the two enzymes were not different. This might have been due to a difference in their initial substrate binding preferences. As very small amounts of G3 and G1 were produced, a small change in substrate binding, which might be detected by G6 hydrolysis, could significantly affect the (G2 − G1)/(G3 + G1) ratio. The lower G2/G3 ratio resulting from G6 hydrolysis by the N282A mutant enzyme indicates that its true (G2 − G1)/(G3 + G1) ratio in FP hydrolysis is higher than the measured ratio, consistent with its higher processivity based on the ratio of soluble reducing sugars to insoluble reducing sugars. The similarity of the two approaches for measuring processivity is further supported by the data for the L230A mutant enzyme. The higher (G2 − G1)/(G3 + G1) ratio of the L230A mutant enzyme is due to its lower initial binding preference leading to G3 as it produced less G3 from G6.

The ratio of oligosaccharides cannot be used to assess processivity in mixtures with endocellulases as G3 is produced by internal cleavage, as well as in the initial hydrolysis step. A different ratio, G2/(G1 + G3) was used to measure processivity for *T. reesei* exocellulase Cel7A (32) as G1 was assumed to be released only from the initial attack (G3 hydrolysis by Cel7A was not addressed in this study). High processivity means that

TABLE 2. Oligosaccharide production with FP and cellohexaose (G6) by Cel6B enzymes[a]

Enzyme	FP hydrolysis (16 h of incubation)				G6 hydrolysis (10 min of incubation)	
	Amt of oligosaccharides (nmol)			(G2 − G1)/(G3 + G1)	Amt of unhydrolyzed G6 (nmol)	G2/G3
	G1	G2	G3			
Wild type	0.22 ± 0.07	3.35 ± 0.07	0.16 ± 0.02	8.2	0.65 ± 0.13	0.97 ± 0.01
L230A	0.33 ± 0.09	9.22 ± 0.02	0.25 ± 0.02	15.3	0.51 ± 0.07	1.14 ± 0.04
N282A	0.22 ± 0.04	8.29 ± 0.04	0.34 ± 0.06	14.4	0.90 ± 0.04	0.86 ± 0.01

[a] Amounts of oligosaccharides were determined by HPLC.

TABLE 3. Synergism of Cel6B enzymes with *T. fusca* endocellulase Cel5A and exocellulase Cel48A in FP and PC hydrolysis

Enzyme or mixture	Molar ratio in mixture	Sp act (μmol cellobiose min^{-1} μmol^{-1} enzyme)[a]	% of wild-type or wild-type mixture activity	Synergism factor[b]	Processivity
FP hydrolysis					
Cel6B		0.22	100		7.2
L230A		0.35	159		9.9
N282A		0.32	145		20.9
Cel5A		0.93			
Cel6B + Cel5A	4:1	2.39	100	6.20	8.4
L230A + Cel5A	4:1	2.41	101	5.45	7.6
N282A + Cel5A	4:1	2.05	86	3.77	5.6
Cel6B + Cel48A	1:1	1.24	100	1.99	7.3
L230A + Cel48A	1:1	1.69	136	3.51	9.6
N282A + Cel48A	1:1	1.45	117	2.82	12.9
Cel6B + Cel48A + Cel5A	4:8:1	6.69	100	6.38	
L230A + Cel48A + Cel5A	4:8:1	5.70	85	4.49	
N282A + Cel48A + Cel5A	4:8:1	2.85	43	3.70	
PC hydrolysis					
Cel6B		3.4	100		
L230A		8.5	252		
N282A		10.6	313		
Cel5A		49.4			
Cel6B + Cel5A	4:1	460	100	3.26	
L230A + Cel5A	4:1	362	79	2.46	
N282A + Cel5A	4:1	289	63	2.24	

[a] The average coefficient of variation was 4%.
[b] Activity of a mixture divided by the sum of the activities of the mixture components.

the enzyme has been optimized for the movement of a cellulose chain in the active site, but this change can reduce hydrolysis activity on easily diffusible soluble substrates (8), which is in agreement with the slow hydrolysis of G6 by the N282A mutant enzyme.

Although the individual mutant enzymes had higher activity with FP than the wild-type enzyme, mixtures of these enzymes with *T. fusca* Cel5A did not show increased synergism with FP.

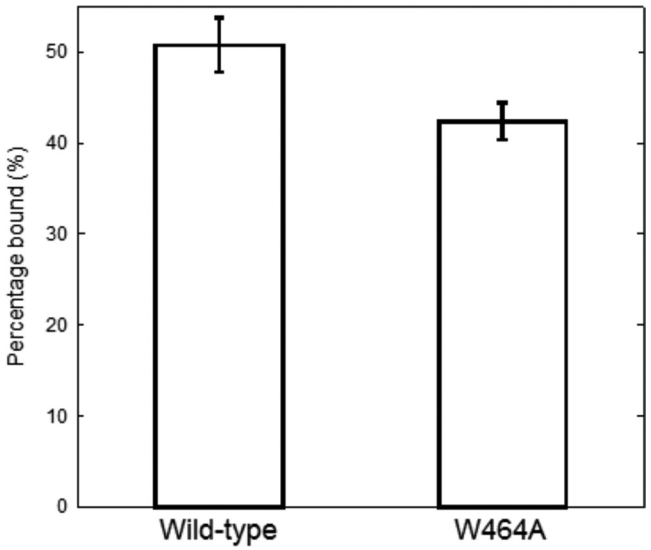

FIG. 2. Binding of wild-type Cel6B and the W464A enzyme to BMCC. Substrate binding was performed using 4 μM enzymes in 50 mM NaOAc (pH 5.5) and 10% glycerol for 1 h at 4°C.

Walker et al. (33) found that there was no binding competition between Cel6B and Cel5A. Jeoh et al. (16), using fluorescently labeled Cel6B and Cel5A, found that the substrate binding of these enzymes in mixtures was greater than that of the individual enzymes. As a very low enzyme-to-substrate ratio was used here, competition for adsorption is unlikely. The fact that the rate of hydrolysis of an exocellulase increased with endocellulase-pretreated cellulose (34) and the fact that synergism occurs between cellulases from unrelated organisms (14) show that synergism does not require a direct interaction between the cellulases. A simple synergism model is that endocellulases act on accessible sites, producing new ends for attack by exocellulases, which in turn open up new sites for endocellulases. However, our data suggested a more complicated synergism, in which a more active exocellulase does not give higher synergism even at low enzyme-to-substrate ratios. As endocellulase Cel5A produces shorter cellulose chains, exocellulase mutants with increase processivity are not needed for maximizing synergism. In contrast, these mutant enzymes did exhibit increased synergism with the reducing-end-attacking exocellulase Cel48A.

Inverse effects on substrates. Activity with CMC is not a good indicator of higher activity with crystalline substrates. Soluble CMC is expected to bind readily in the active site, but its high proportion of modified residues may cause CMC to bind in a distorted manner. The tunnel structure of *H. insolens* Cel6A restricts the polysaccharide strand in the tunnel (31), so the increased activity of the W464A enzyme with CMC might be due to easier movement of modified sugars through the tunnel after removal of the bulky side chain. Increased activity with CMC and decreased activity with BMCC have also been

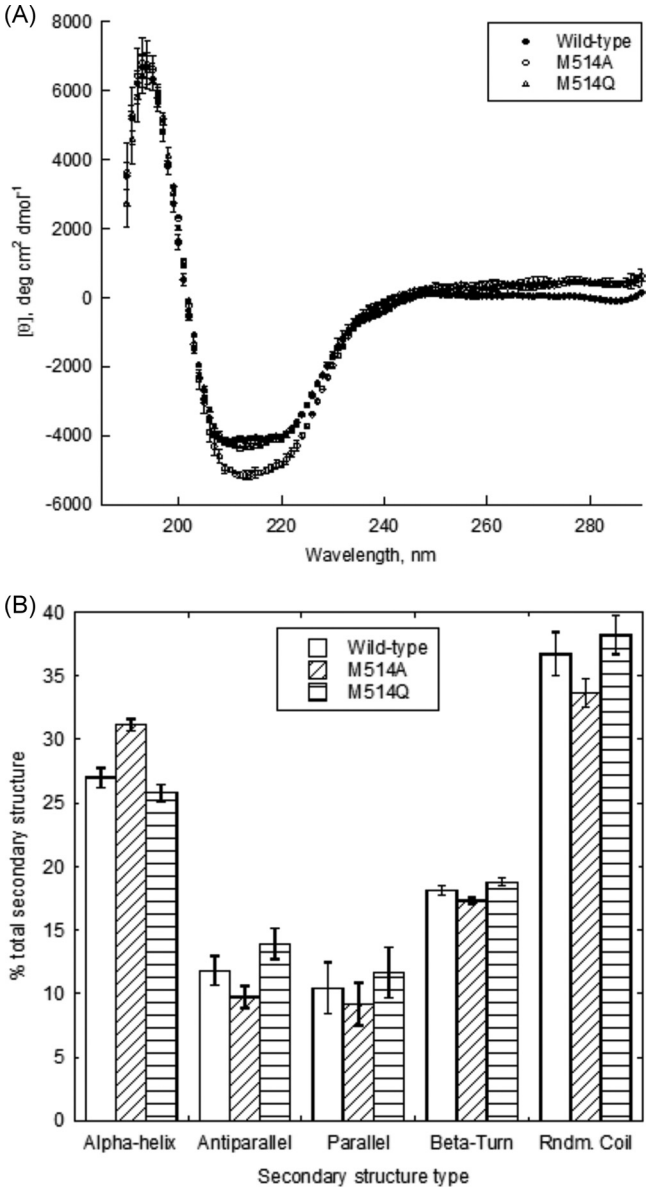

FIG. 3. CD analysis. (A) CD spectra of wild-type Cel6B and the M514A and M514Q mutant enzymes. (B) Relative amount of each type of secondary structure of each enzyme. The error bars represent the standard deviations for three independent trials.

observed for several *T. fusca* Cel9A mutations (19) when substrate-binding Trp residues were mutated to smaller side chains.

The decrease in both activity and binding to BMCC caused by the W464A mutation indicates that W464 helps to bind a cellulose chain to the active site and that this function may not be required for binding of easy accessible substrates like CMC and PC. Structural analysis showed that the corresponding residue in *T. reesei* Cel6A, W367, interacts with the α-face of a glucosyl ring during productive binding of a cellulose chain (23), and the position of *H. insolens* Cel6A W371 was shifted upon ligand binding (28).

The specific loss of activity of the M514 mutant enzymes with BMCC during storage suggests that a change in structure occurs during storage that inactivates the rate-limiting step for activity with crystalline cellulose. Residue M514 is located in a tunnel-forming loop at subsite +1, next to residue C515, which forms a disulfide bond with residue C465 in this loop. The flexibility of this disulfide bond might cause a conformational change, as shown by CD and reduced thermostability.

In conclusion, *T. fusca* Cel6B was mutated to enhance activity with selected substrates, but improving exocellulase activity by increasing processivity is not always an effective strategy to achieve higher synergism between exocellulases and endocellulases with crystalline cellulose.

ACKNOWLEDGMENTS

This work was supported by the Vietnam Education Foundation and by grant DE-FG02-ER15356 from the U.S. Department of Energy.

We gratefully acknowledge the helpful assistance of Diana Irwin, Cornell University. We thank Jessica Hatch and Arthur Stipanovic, Department of Chemistry, SUNY College of Environmental Science and Forestry, for structural analysis of SC and PC and Jose Moran-Mirabal, Biofuels Research Laboratory, Department of Biological and Environmental Engineering, Cornell University, for assistance with HPLC.

REFERENCES

1. **Arnold, K., L. Bordoli, J. Kopp, and T. Schwede.** 2006. The SWISS-MODEL workspace: a web-based environment for protein structure homology modelling. Bioinformatics **22:**195–201.
2. **Bayer, E. A., H. Chanzy, R. Lamed, and Y. Shoham.** 1998. Cellulose, cellulases and cellulosomes. Curr. Opin. Struct. Biol. **8:**548–557.
3. **Bhat, M. K., and S. Bhat.** 1997. Cellulose degrading enzymes and their potential industrial applications. Biotechnol. Adv. **15:**583–620.
4. **Bohm, G., R. Muhr, and R. Jaenicke.** 1992. Quantitative analysis of protein far UV circular dichroism spectra by neural networks. Protein Eng. **5:**191–195.
5. **Clarke, A. J.** 1996. Biodegradation of cellulose. Enzymology and biotechnology. Technomic Publishing Company, Lancaster, PA.
6. **Davies, G. J., A. M. Brzozowski, M. Dauter, A. Varrot, and M. Schulein.** 2000. Structure and function of *Humicola insolens* family 6 cellulases: structure of the endoglucanase, Cel6B, at 1.6Å resolution. Biochem. J. **348:**201–207.
7. **Ghose, T. K.** 1987. Measurement of cellulase activities. Pure Appl. Chem. **59:**257–268.
8. **Harjunpaa, V., A. Teleman, A. Koivula, L. Ruohonen, T. T. Teeri, O. Teleman, and T. Drakenberg.** 1996. Cello-oligosaccharide hydrolysis by cellobiohydrolase II from *Trichoderma reesei.* Association and rate constants derived from an analysis of progress curves. Eur. J. Biochem. **240:**584–591.
9. **Heinzelman, P., C. D. Snow, I. Wu, C. Nguyen, A. Villalobos, S. Govindarajan, J. Minshull, and F. H. Arnold.** 2009. A family of thermostable fungal cellulases created by structure-guided recombination. Proc. Natl. Acad. Sci. USA **106:**5610–5615.
10. **Henrissat, B., H. Driguez, C. Viet, and M. Schulein.** 1985. Synergism of cellulases from *Trichoderma reesei* in the degradation of cellulose. Nat. Biotechnol. **3:**722–726.
11. **Hooft, R. W. W., G. Vriend, C. Sander, and E. E. Abola.** 1996. Errors in protein structures. Nature **381:**272.
12. **Horn, S. J., P. Sikorski, J. B. Cederkvist, G. Vaaje-Kolstad, M. Sorlie, B. Synstad, G. Vriend, K. M. Varum, and V. G. Eijsink.** 2006. Costs and benefits of processivity in enzymatic degradation of recalcitrant polysaccharides. Proc. Natl. Acad. Sci. USA **103:**18089–18094.
13. **Horn, S. J., A. Sorbotten, B. Synstad, P. Sikorski, M. Sorlie, K. M. Varum, and V. G. H. Eijsink.** 2006. Endo/exo mechanism and processivity of family 18 chitinases produced by *Serratia marcescens*. FEBS J. **273:**491–503.
14. **Irwin, D. C., M. Spezio, L. P. Walker, and D. B. Wilson.** 1993. Activity studies of eight purified cellulases: specificity, synergism, and binding domain effects. Biotechnol. Bioeng. **42:**1002–1013.
15. **Irwin, D. C., S. Zhang, and D. B. Wilson.** 2000. Cloning, expression and characterization of a family 48 exocellulase, Cel48A, from *Thermobifida fusca*. Eur. J. Biochem. **267:**4988–4997.
16. **Jeoh, T., D. B. Wilson, and L. P. Walker.** 2002. Cooperative and competitive binding in synergistic mixtures of *Thermobifida fusca* cellulases Cel5A, Cel6B, and Cel9A. Biotechnol. Prog. **18:**760–769.
17. **Jung, E. D., G. Lao, D. Irwin, B. K. Barr, A. Benjamin, and D. B. Wilson.** 1993. DNA sequences and expression in *Streptomyces lividans* of an exoglucanase gene and an endoglucanase gene from *Thermomonospora fusca*. Appl. Environ. Microbiol. **59:**3032–3043.

18. **Koivula, A., L. Ruohonen, G. Wohlfahrt, T. Reinikainen, T. T. Teeri, K. Piens, M. Claeyssens, M. Weber, A. Vasella, D. Becker, M. L. Sinnott, J. Y. Zou, G. J. Kleywegt, M. Szardenings, J. Stahlberg, and T. A. Jones.** 2002. The active site of cellobiohydrolase Cel6A from *Trichoderma reesei*: the roles of aspartic acids D221 and D175. J. Am. Chem. Soc. **124:**10015–10024.
19. **Li, Y., D. C. Irwin, and D. B. Wilson.** 2007. Processivity, substrate binding, and mechanism of cellulose hydrolysis by *Thermobifida fusca* Cel9A. Appl. Environ. Microbiol. **73:**3165–3172.
20. **Lynd, L. R., P. J. Weimer, W. H. van Zyl, and I. S. Pretorius.** 2002. Microbial cellulose utilization: fundamentals and biotechnology. Microbiol. Mol. Biol. Rev. **66:**506–577.
21. **Pages, S., H. C. Kester, J. Visser, and J. A. Benen.** 2001. Changing a single amino acid residue switches processive and non-processive behavior of *Aspergillus niger* endopolygalacturonase I and II. J. Biol. Chem. **276:**33652–33656.
22. **Percival Zhang, Y. H., M. E. Himmel, and J. R. Mielenz.** 2006. Outlook for cellulase improvement: screening and selection strategies. Biotechnol. Adv. **24:**452–481.
23. **Rouvinen, J., T. Bergfors, T. Teeri, J. K. Knowles, and T. A. Jones.** 1990. Three-dimensional structure of cellobiohydrolase II from *Trichoderma reesei*. Science **249:**380–386.
24. **Rubin, E. M.** 2008. Genomics of cellulosic biofuels. Nature **454:**841–845.
25. **Shimada, M., and M. Takahashi.** 1991. Biodegradation of cellulosic materials, p. 621–663. *In* D. N. S. Hon and N. Shiraishi (ed.), Wood and cellulosic chemistry. Marcel Dekker, New York, NY.
26. **Spezio, M., D. B. Wilson, and P. A. Karplus.** 1993. Crystal structure of the catalytic domain of a thermophilic endocellulase. Biochemistry **32:**9906–9916.
27. **Tarchevsky, I. A., and G. N. Marchenko.** 1991. Cellulose: biosynthesis and structure. Springer-Verlag, New York, NY.
28. **Varrot, A., T. P. Frandsen, I. von Ossowski, V. Boyer, S. Cottaz, H. Driguez, M. Schulein, and G. J. Davies.** 2003. Structural basis for ligand binding and processivity in cellobiohydrolase Cel6A from *Humicola insolens*. Structure **11:**855–864.
29. **Varrot, A., S. Hastrup, M. Schulein, and G. J. Davies.** 1999. Crystal structure of the catalytic core domain of the family 6 cellobiohydrolase II, Cel6A, from *Humicola insolens*, at 1.92Å resolution. Biochem. J. **337:**297–304.
30. **Varrot, A., S. Leydier, G. Pell, J. M. Macdonald, R. V. Stick, B. Henrissat, H. J. Gilbert, and G. J. Davies.** 2005. *Mycobacterium tuberculosis* strains possess functional cellulases. J. Biol. Chem. **280:**20181–20184.
31. **Varrot, A., M. Schulein, and G. J. Davies.** 1999. Structural changes of the active site tunnel of *Humicola insolens* cellobiohydrolase, Cel6A, upon oligosaccharide binding. Biochemistry **38:**8884–8891.
32. **von Ossowski, I., J. Ståhlberg, A. Koivula, K. Piens, D. Becker, H. Boer, R. Harle, M. Harris, C. Divne, S. Mahdi, Y. Zhao, H. Driguez, M. Claeyssens, M. L. Sinnott, and T. T. Teeri.** 2003. Engineering the exo-loop of *Trichoderma reesei* cellobiohydrolase, Cel7A. A comparison with *Phanerochaete chrysosporium* Cel7D. J. Mol. Biol. **333:**817–829.
33. **Walker, L. P., C. D. Belair, D. B. Wilson, and D. C. Irwin.** 1993. Engineering cellulase mixtures by varying the mole fraction of *Thermomonospora fusca* E5 and E3, *Trichoderma reesei* CBHI, and *Caldocellum saccharolyticum* glucosidase. Biotechnol. Bioeng. **42:**1019–1028.
34. **Wilson, D. B., and D. C. Irwin.** 1999. Genetics and properties of cellulases, p. 1–21. *In* T. Scheper (ed.), Advances in biochemical engineering/biotechnology, vol. 65. Springer-Verlag, Heidelberg, Germany.
35. **Zhang, S., D. C. Irwin, and D. B. Wilson.** 2000. Site-directed mutation of noncatalytic residues of *Thermobifida fusca* exocellulase Cel6B. Eur. J. Biochem. **267:**3101–3115.
36. **Zhang, S., G. Lao, and D. B. Wilson.** 1995. Characterization of a *Thermomonospora fusca* exocellulase. Biochemistry **34:**3386–3395.
37. **Zhang, Y. H., and L. R. Lynd.** 2004. Toward an aggregated understanding of enzymatic hydrolysis of cellulose: noncomplexed cellulase systems. Biotechnol. Bioeng. **88:**797–824.
38. **Zhang, Y. H. P., J. Cui, L. R. Lynd, and L. R. Kuang.** 2006. A transition from cellulose swelling to cellulose dissolution by *o*-phosphoric acid: evidence from enzymatic hydrolysis and supramolecular structure. Biomacromolecules **7:**644–648.
39. **Zhou, W., D. C. Irwin, J. Escovar-Kousen, and D. B. Wilson.** 2004. Kinetic studies of *Thermobifida fusca* Cel9A active site mutant enzymes. Biochemistry **43:**9655–9663.